17th World Conference on Earthquake Engineering, 17WCEE
Sendai, Japan - September 13th to 18th 2020

SIMPLIFIED ANALYSIS OF REINFORCED CONCRETE SHEAR PANEL ELEMENTS UNDER STATIC LOADS USING MODIFIED FSAM

N. Thammishetti[1], SS Prakash[2], J. Hashemi[3], R. Al-Mahaidi[4]

[1] *IITH-SUT Joint PhD candidate, Indian Institute of Technology Hyderabad, ce16resch11005@iith.ac.in*
[2] *Associate Professor, Indian Institute of Technology Hyderabad, suriyap@iith.ac.in*
[3] *Senior Lecturer, Swinburne University of Technology, Hawthorn, jhashemi@swin.edu.au*
[4] *Professor, Swinburne University of Technology, Hawthorn, ralmahaidi@swin.edu.au*

Abstract

During earthquakes, reinforced concrete (RC) structures are typically subjected to high shear loading. The reliable estimate of the behaviour of RC members under shear loads depends on the analytical model used. This work focuses on the analytical modelling of RC shear panel elements, which is essential for the full understanding of member-level shear behaviour. A fixed strut angle model (FSAM) was initially proposed for predicting the shear behaviour of RC panel elements. FSAM was later modified to consider the effect of dowel action and aggregate interlock. However, the modified model uses empirical constitutive relationships to incorporate the contributions of the dowel and aggregate interlock to shear resistance. Moreover, the existing FSAM discards the contribution of aggregate interlock when the stresses normal to cracks are tensile. Neglecting aggregate interlock resistance under open crack conditions causes convergence difficulties in the solution algorithm of FSAM in the post yield regime. This paper presents a modified FSAM approach employing experimentally validated constitutive relationships for modelling the aggregate interlock mechanism. Extensive validation studies considering variations in the longitudinal and transverse steel reinforcement ratios and concrete strength were carried out to understand the efficacy of the proposed model. Predictions of the modified FSAM in the post-yield regime are better than those of the original model. The modified model also predicts the overall response of the shear panel with reasonable accuracy.

Keywords: biaxial loads, flexure-shear, FSAM, panel model, reinforced concrete, shear

1. Introduction

A reasonable estimate of overall behaviour can be achieved based on the understanding of the behaviour of individual RC membrane elements subjected to multi-axial stresses. The axial and flexural effects can be relatively well understood through the sectional analysis of RC members using uniaxial fibres. However, the shear behaviour of RC elements is a two-dimensional problem. The interaction effects of shear loads with axial and flexural loads are complex. Previously, many membrane models using the smeared crack approach were developed based on the results of shear panel testing in order to understand the shear behaviour of cracked RC membrane elements. The smeared crack shear models developed over the past three decades include, but are not limited to, the diagonal compression field theory (DCFT) [1] , the compression field theory (CFT) [2] , the modified compression field theory (MCFT) [3] , the rotating-angle softened truss model (RA-STM) [4] , the fixed angle softened truss model (FA-STM) [5] , the disturbed stress field model (DSFM) [6] , and the softened membrane model (SMM) [7] . The models developed have achieved different levels of success in predicting the load-displacement behaviour of RC elements subjected to different combined loading actions[8]

Considering the complexity involved in implementing the existing models in fibre-based macroscopic models, Ulugtekin (2010) proposed a simple fixed-strut angle model (FSAM) [9] The model was later modified to take into account the shear aggregate interlock [10] . As the shear aggregate interlock was considered only when the crack was closed, it led to zero shear stiffness along open cracks, resulting in discrepancies in the predicted member behaviour. Kolozvari et al. (2015), later implemented FSAM in SFI-MVLEM, including dowel action on reinforcing bars as the shear mechanism which provides shear resistance even when the crack is open [11] .

2. Research Significance

The shear mechanisms used in the existing FSAM are shear aggregate interlock and dowel action, and both mechanisms are modelled using empirical relationships. The model considers the shear stiffness at cracking through the dowel action. However, discarding the shear aggregate interlock when the crack cannot be related to the physical behaviour of the member. The parameters of the empirical relationships are obtained based on calibration studies. Considering the drawbacks of the existing FSAM, the aim of the present study is to incorporate a shear aggregate model developed based on experimental validation which includes the shear resistance provided by interlock even when the crack is open.

3. Background to Original Fixed Sturt Angle Model (FSAM)

The behaviour of the panel element under shear loading can be divided into three phases as follows: (a) uncracked panel behaviour, (b) behaviour after the formation of the first crack and (c) behaviour after the formation of the second crack.

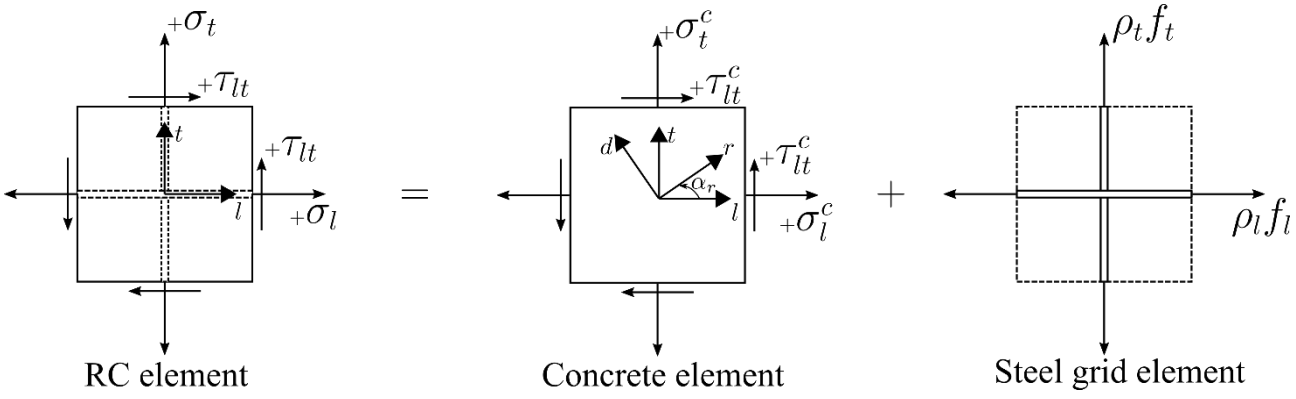

Figure 1 Uncracked behaviour of panel

3.1 Uncracked behaviour

Figure 1 illustrates the stresses acting on the components of an RC membrane element subjected to in-plane shear and normal stresses. The directions of the longitudinal and transverse steel bars are designated as the 'l' and 't' axis, respectively. The normal stresses are designated as σ_l and σ_t in the l and t directions, respectively. The shear stresses are represented by τ_{lt} in the $l-t$ coordinate system. The angle between the direction of the principal tensile stress (r-axis) and the direction of the longitudinal steel (l-axis) is defined as the rotating angle α_r, which is dependent on the relative amount of smeared steel stresses ($\rho_l f_l$ and $\rho_t f_t$) in the longitudinal and transverse directions. Assuming that the direction of principal stresses coincides with the direction of principal strains, the equilibrium and compatibility equations for uncracked behaviour can be written as shown in Eqs. (1) - (6)

Equilibrium equations:

$$\sigma_l = \sigma_r \cos^2 \alpha_r + \sigma_d \sin^2 \alpha_r + \rho_l f_l \quad (1)$$

$$\sigma_t = \sigma_r \sin^2 \alpha_r + \sigma_d \cos^2 \alpha_r + \rho_t f_t \quad (2)$$

$$\tau_{lt} = (\sigma_r - \sigma_d) \sin \alpha_r \cos \alpha_r \quad (3)$$

Compatibility equations:

$$\varepsilon_l = \varepsilon_r \cos^2 \alpha_r + \varepsilon_d \sin^2 \alpha_r \quad (4)$$

$$\varepsilon_t = \varepsilon_r \sin^2 \alpha_r + \varepsilon_d \cos^2 \alpha_r \quad (5)$$

$$\frac{\gamma_{lt}}{2} = (\varepsilon_r - \varepsilon_d) \sin \alpha_r \cos \alpha_r \quad (6)$$

3.2 Behaviour after the formation of the first crack

When the principal tensile stress reaches the tensile strength of concrete, cracks form, and separate the concrete into a series of struts. After the formation of the first crack, the applied stresses are resisted by the forces in the strut (Figure 2). The angle between the direction of the strut and the direction of the longitudinal steel (l-axis) is defined as the fixed strut angle α1 and the strut angle remains unchanged through the course of loading. The equilibrium and compatibility equations for cracked behaviour are shown below in Eqs. (7) – (12)

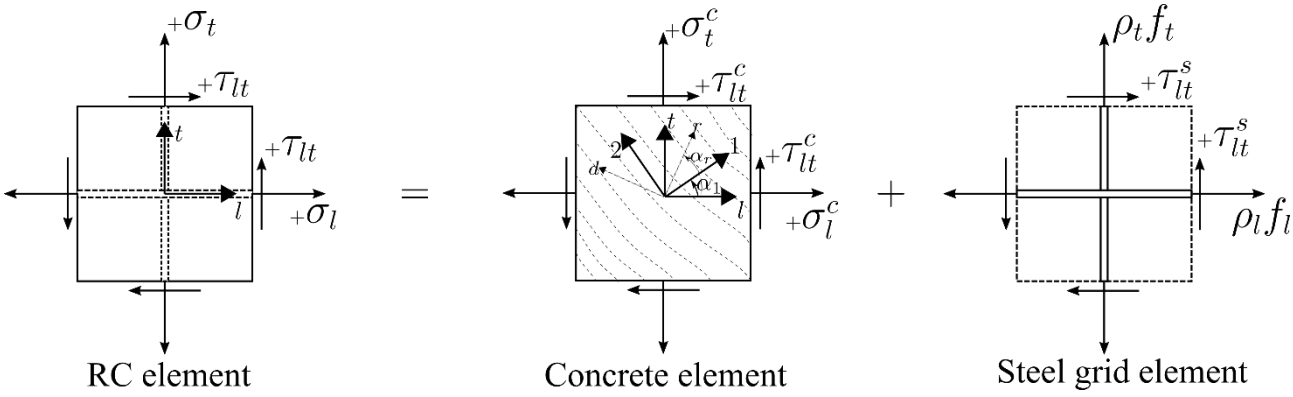

Figure 2 Behaviour of the panel after the formation of the first crack

Equilibrium equations:

$$\sigma_l = \sigma_1^c \cos^2 \alpha_1 + \sigma_2^c \sin^2 \alpha_1 - \tau_{12}^c 2 \sin \alpha_1 \cos \alpha_1 + \rho_l f_l \quad (7)$$

$$\sigma_t = \sigma_1^c \sin^2 \alpha_1 + \sigma_2^c \cos^2 \alpha_1 + \tau_{12}^c 2 \sin \alpha_1 \cos \alpha_1 + \rho_t f_t \quad (8)$$

$$\tau_{lt} = (\sigma_1^c - \sigma_2^c) \sin \alpha_1 \cos \alpha_1 + \tau_{12}^c (\cos^2 \alpha_1 - \sin^2 \alpha_1) + \tau_{lt}^s \quad (9)$$

Compatibility equations:

$$\varepsilon_l = \varepsilon_1 \cos^2 \alpha_1 + \varepsilon_2 \sin^2 \alpha_1 - \frac{\gamma_{12}}{2} 2 \sin \alpha_1 \cos \alpha_1 \quad (10)$$

$$\varepsilon_t = \varepsilon_1 \sin^2 \alpha_1 + \varepsilon_2 \cos^2 \alpha_1 + \frac{\gamma_{12}}{2} 2 \sin \alpha_1 \cos \alpha_1 \quad (11)$$

$$\frac{\gamma_{lt}}{2} = (\varepsilon_1 - \varepsilon_2) \sin \alpha_1 \cos \alpha_1 + \frac{\gamma_{12}}{2} (\cos^2 \alpha_1 - \sin^2 \alpha_1) \quad (12)$$

4. Material Models

The constitutive material models employed for the analysis of RC membrane elements are presented in this section.

4.1 Concrete:

The softened compression response of concrete proposed by Chang and Mander (1994) [12] is considered to model the compressive stress-strain behaviour of concrete. The compression model is defined by Eqs. (13) – (18)

Compression Model:

$$\varepsilon_0 = \frac{\sqrt[4]{f_c'}}{1150}, \mathrm{r} = \frac{f_c'}{5.2} - 1.9, \mathrm{m} = \frac{7.2}{f_c'^{\frac{3}{8}}}, \mathrm{x} = \frac{\varepsilon_c}{\varepsilon_0} \quad (13)$$

$$D = 1 + (m - 1 + log\, x)x, \quad for\, r = 1 \quad (14)$$

$$D = 1 + \left(m - \frac{r}{r-1}\right) x + \frac{x^r}{r-1} \quad (15)$$

Softening Coefficient:

$$K_c = 0.27 \left(\frac{\varepsilon_r}{\varepsilon_0} - 0.37\right) \geq 1 \quad (16)$$

$$\beta = \frac{1}{1 + K_c} \quad (17)$$

$$\sigma_c = \beta \frac{f_c' n x}{D} \quad (18)$$

The tension stiffening model proposed by Belarbi and Hsu (1994) [13] presented below (Eqs. (19) – (24)) is used to model the tension behaviour of concrete

Tension Model:

$$E_c = 3875 (f_c')^{0.5} \quad (19)$$

$$f_{cr} = 0.31 (f_c')^{0.5} \quad (20)$$

$$\varepsilon_{cr} = 0.00008 \quad (21)$$

$$\sigma_{ct} = E_c \varepsilon_{ct}; for \quad \varepsilon_{ct} \leq \varepsilon_{cr} \quad (22)$$

$$\sigma_{ct} = f_{cr} \left(\frac{\varepsilon_{cr}}{\varepsilon_{ct}}\right)^{0.4} \quad (23)$$

Effective yield strength:

$$f_{yeff} = f_y \left[1 - 1.314 \frac{n^{0.434}}{\rho^{1.084}} \left(\frac{f_{cr}}{f_y}\right)^{1.517}\right] \quad (24)$$

4.2 Steel

The stress-strain response of steel originally developed by Menegotto and Pinto (1973) [14] and later modified is used to model the compression and tension behaviour of steel

Compression and Tension:

The uniaxial monotonic stress-strain relationship for reinforcing steel takes the form:

$$\varepsilon_y = \frac{f_y}{E_s}, \varepsilon^* = \frac{\varepsilon_s}{\varepsilon_y}, R_0 = 20, \tag{25}$$

$$f_s = \varepsilon_s f_y \left(b\varepsilon^* + \frac{(1-b)\varepsilon^*}{(1+\varepsilon^* R_0)^{\frac{1}{R_0}}} \right) \tag{26}$$

where, b is the strain hardening parameter and R_0 is the curvature parameter.

The strain hardening parameter and the curvature parameter can be calibrated to describe experimental behaviour. In the present study, values of 0.0001 and 20 are considered for b and R_0, respectively.

5. Shear Transfer Mechanisms

The primary modes of shear transfer along the crack plane are the shear resistance provided by the interlocking of aggregate along the crack (Figure 3), and the dowel resistance developed due to the curvature induced in steel in the vicinity of the crack locations. The following sub-sections present details of the shear aggregate interlock and dowel action mechanisms implemented in the modelling.

5.1 Original Fixed Strut Angle Model

A simple friction-based shear aggregate interlock model and a linear-elastic model describing the shear resistance of reinforcing bars are considered for RC panel behaviour in the original FSAM model. These formulations are discussed in detail below:

5.1.1 Aggregate shear interlock

Orakcal et al. (2012) proposed a friction-based constitutive relationship to model the effects of shear aggregate interlock [9]. The model has the following inherent assumptions:

- The shear transferred across the cracks is set to zero when the concrete stresses perpendicular to the crack are tensile. This assumption essentially leads to zero shear transfer when the cracks are open.
- The shear strain vs. sliding strain varies linearly. The elastic stiffness of shear stress vs. sliding strain is presumed to be a fraction of concrete elastic modulus.

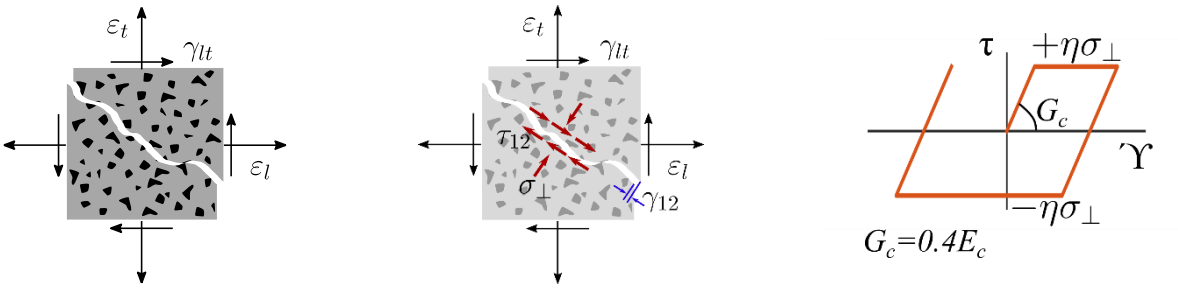

(a) Cracked concrete (b) Aggregate interlock mechanism (c) Shear aggregate interlock model

Figure 3 Aggregate interlock mechanism

As the approach considers the shear transfer across cracks through the shear-friction mechanism, the shear stress is capped to a fraction of the compressive concrete stress perpendicular to cracks. Under constant compressive concrete stress in concrete perpendicular to the crack, the friction-based model generates an elastoplastic behaviour when subjected cyclic sliding strain, as shown in Figure 3.

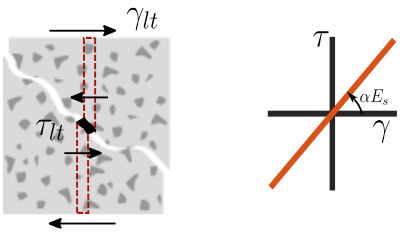

Figure 4 Dowel action model in FSAM

5.1.2 Dowel action

Consideration of zero-shear transfer across the cracks when the stresses normal to the crack are tensile leads to zero shear stiffness in the membrane. To model the behaviour of the membrane, Kolozvari (2013) proposed a linear-elastic constitutive relationship to consider the effect of dowel action in the membrane element [15] The model considers the stiffness of the dowel response to be a fraction of the elastic modulus of steel. The relationship between the dowel shear stress in steel to the shear strain is given in Equation 27 below. As the shear resisting mechanisms considered in FSAM are based on empirical relationships, sensitivity analysis is performed to obtain the friction coefficient η and dowel action parameter α.

$$\tau_{lt} = \alpha\, E_s \gamma_{lt} \tag{27}$$

5.2 Modified FSAM (MFSAM)

The present study proposes the use of the aggregate interlock model proposed by Bujadham and Maekawa (1992) [16] which is based on the Universal Stress Transfer Model. The shear transfer mechanism in the cracked concrete is modelled using the aggregate shear interlock model proposed by Maekawa et al. (2003)[17]

$$m = 3.83 f_c^{\frac{1}{3}},\ \varphi = \frac{\gamma_{12}}{\varepsilon_1} \tag{28}$$

$$\tau_{agg} = \frac{m\varphi^2}{1+\varphi^2} \tag{29}$$

$$\sigma_{cagg} = m\left[\frac{\pi}{2} - cot^{-1}\varphi - \frac{\varphi}{1+\varphi^2}\right] \tag{30}$$

Table 1 Details of specimens validated

Specimen ID	Longitudinal steel		Transverse steel		Concrete	Steel ratio	Steel stress ratio
	ρ_l (%)	f_{ly} (MPa)	ρ_t (%)	f_{ty} (MPa)	f_c (MPa)	$\frac{\rho_l}{\rho_t}$	$\frac{\rho_l f_{ly}}{\rho_t f_{ty}}$
A1	0.596	444.80	0.596	444.80	-42.20	1.00	1.00
A2	1.193	462.65	1.193	462.65	-41.23	1.00	1.00
A3	1.789	446.45	1.789	446.45	-41.65	1.00	1.00
B2	1.789	446.45	1.193	462.65	-44.06	1.50	1.45
VB1	2.39	409	1.2	445	-98.2	1.99	1.83
VB4	1.8	455	0.6	445	-96.9	3.00	3.07

6. Experimental Corroboration

In order to ascertain the efficacy of the modified FSAM, the behaviour of RC panel elements subjected to pure shear was predicted using the MFSAM and compared with the test results. In this research, a total of six specimens with different material and cross-sectional properties tested by Pang and Hsu (1995) [4] , Zhang and Hsu (1998) [18] were validated. The main parameters considered were the strength of concrete and the amount of reinforcement. The details of the shear panels validated in this research are presented in Table 1.

For the panels subjected to pure shear, based on close observation of the equilibrium equations 1-3 and 7-9, it is evident that the contribution of dowel action affects the overall shear behaviour and does not influence the equilibrium criteria of zero axial stresses. Based on the above observation, the dowel parameter was set to zero for the validation of the specimens.

7. Discussion of Results

The comparison of experimental results with the analytical results is presented in Figure 5-10. For specimens A1, A2 and A3 which were reinforced with equal amounts of reinforcement in the longitudinal and transverse directions, the predictions from FSAM and MFSAM are relatively similar. Figure 5 illustrates the comparison of analytical prediction and the experimental behaviour of specimen A1. Although the models capture the overall behaviour quite well, they over-estimate the cracking load. The model results can be improved further by calibrating the material models to reflect the experimental behaviour. The analytical estimates of cracking load, peak load and overall behaviour for specimens A2 and A3 (Figure 6-7) are in good agreement with the experimental results. However, the models under-estimate the post-cracking stiffness of specimen A3. Due to the presence of a low and equal amount of reinforcement in both the longitudinal and transverse directions led to the yielding of the reinforcement. The yielding of reinforcement limits the capacity of the shear panel, which is quite well predicted by the analytical models.

The comparison of experimental results with the analytical results of specimens with unequal reinforcement in the transverse and longitudinal directions is presented in Figure 8-10. The FSAM model considers a friction-based shear aggregate interlock mechanism when the cracks are closed. The zero-shear transfer assumption considered by the FSAM model leads to loss of convergence after the yielding of transverse reinforcement, limiting the predictions of FSAM to the load corresponding to the yielding of transverse reinforcement. The MFSAM predictions for specimen B2 reflect the experimentally observed response. Figure 8 (b) and (c) present the variation of stresses in steel with the increase in loading. The stresses in steel are limited to the yielding of transverse steel for the FSAM predictions as convergence is lost with subsequent loading. A similar phenomenon is observed for specimens VB1 and VB4.

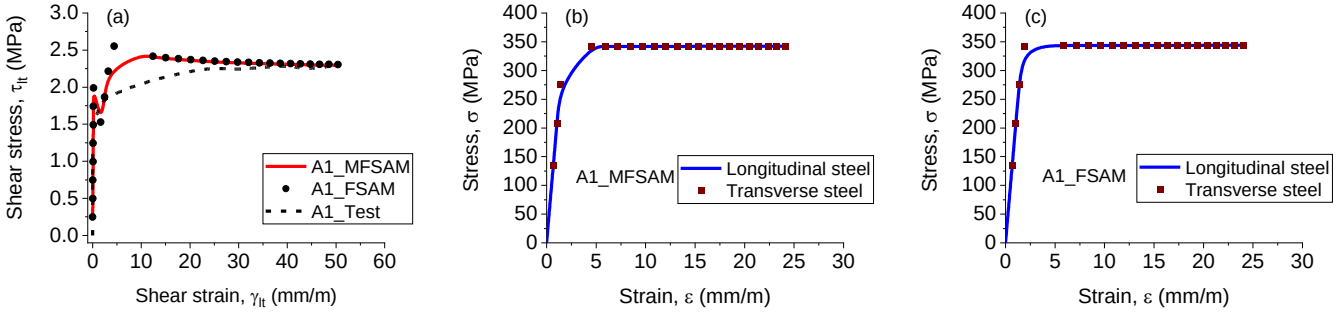

Figure 5 Validation of A1 specimen

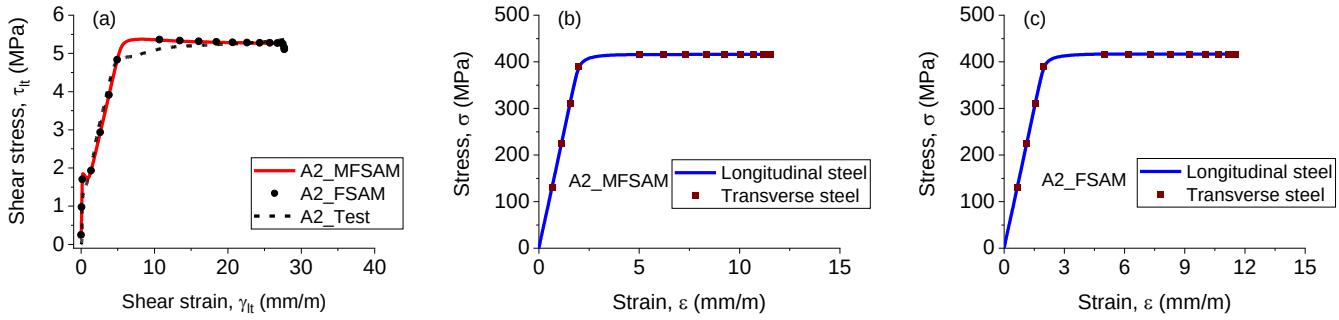

Figure 6 Validation of A2 specimen

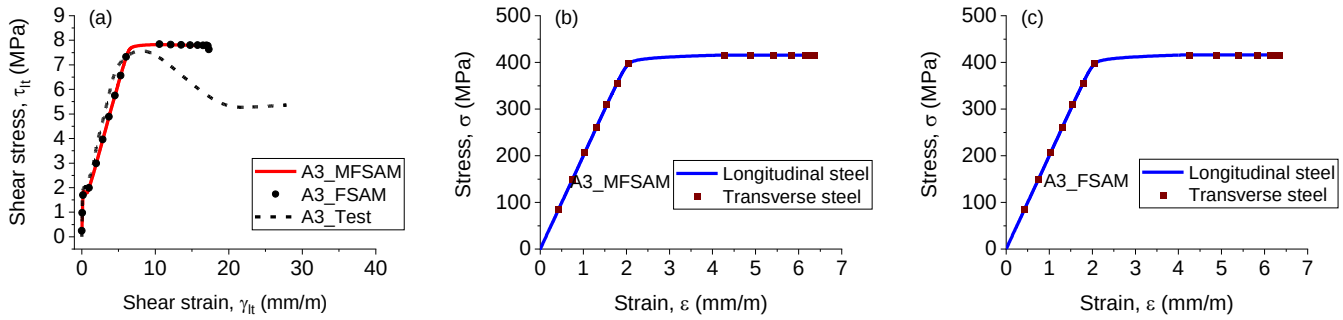

Figure 7 Validation of A3 specimen

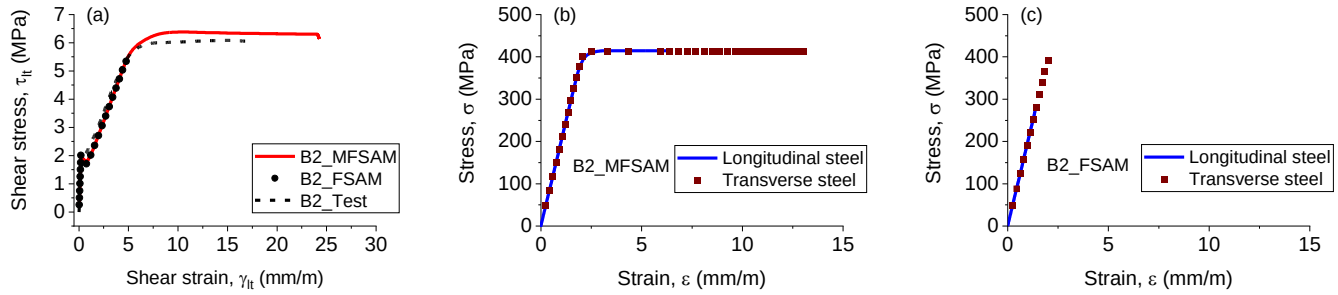

Figure 8 Validation of B2 specimen

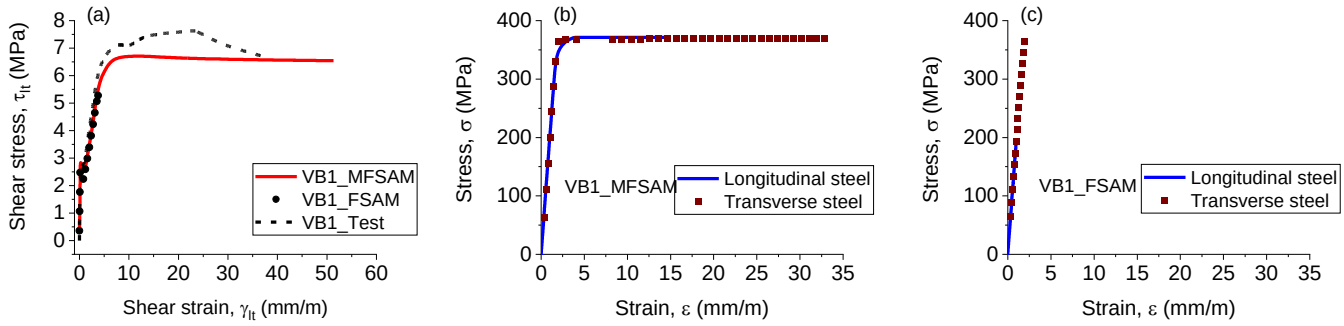

Figure 9 Validation of VB1 specimen

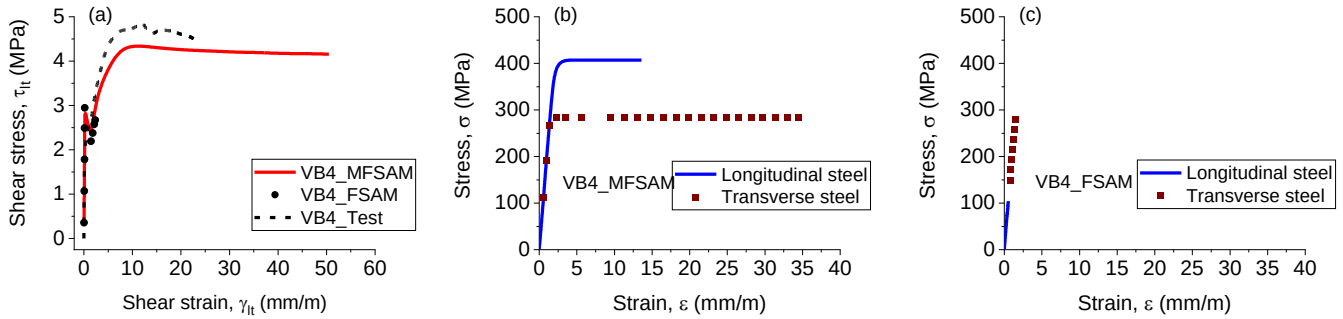

Figure 10 Validation of VB4 specimen

To understand the efficacy of the proposed model in estimating the behaviour of shear panels with high compressive strength, panel specimens VB1 (Figure 9) and VB4 (Figure 10) were validated in this study. Owing to the high strength of concrete, the specimens have a high shear capacity, which is estimated by the

MFSAM model quite well. In addition, the MFSAM model predicts the behaviour quite well until the yielding of transverse steel. The deviation in the predictions after the yielding is attributed to the use of normal-strength concrete model instead of high-strength concrete.

8. Summary and Conclusions

The aim of this study was to improve the existing fixed strut angle model (FSAM) by incorporating the experimentally verified aggregate shear interlock model. Calibration and validation of the proposed modelling approach were conducted using detailed experimental data on specimens with different reinforcement schemes and concrete strengths. The modified FSAM model is able to capture the behaviour of the tested panels quite accurately. The following major conclusions can be drawn based on the results presented in this work.

- The FSAM model provides a reasonable estimate for the monotonic behaviour of RC panels with equal reinforcement in transverse and longitudinal directions.
- The modified FSAM provides accurate predictions of the monotonic behaviour of the shear panel, such as shear stress versus shear strain, and local deformations including normal strains of reinforcing bars in the two orthogonal directions.

9. Acknowledgements

This analytical work was carried out as part of a project funded by SERB, Department of Science and Technology, India. grant No SB/S3/CEE/0060/2013. Their financial support is gratefully acknowledged. The authors also acknowledge the support provided by IITH and SUT to Mr Nikesh Thammishetti through the IITH-SUT Joint PhD program.

Nomenclature

E_c	Elastic modulus of concrete
E_s	Elastic modulus of steel
R_0	Curvature parameter
b	Strain hardening parameter
n	The ratio of E_s to E_c
f_c'	Compressive strength of concrete
f_{cr}	Cracking stress of concrete
f_l	Stress in longitudinal steel
f_{ly}	Yield stress of longitudinal steel
f_s	Stress in steel
f_t	Stress in transverse steel
f_{ty}	Yield stress of transverse steel
f_y	Yield stress of steel
f_{yeff}	Effective yield stress of steel
α	Dowel action parameter
α_1	The angle of strut
α_r	The direction of principal strain
β	Concrete softening coefficient
γ_{12}	Shear strain in the concrete strut
γ_{lt}	Shear strain in RC panel
ε_0	Strain corresponding to peak stress in concrete
ε_1	Tensile strain in the concrete strut
ε_2	Compressive strain in the concrete strut
ε_c	Compressive strain in concrete
ε_{cr}	Cracking strain of concrete
ε_{ct}	Tensile strain in concrete
ε_d	Principal compressive strain in concrete
ε_l	Longitudinal strain in RC panel
ε_r	Principal tensile strain in concrete
ε_t	Transverse strain in RC panel
ε_y	Strain corresponding to yielding to steel
η	Shear aggregate interlock parameter
ρ	Reinforcement ratio
ρ_l	Longitudinal steel ratio
ρ_t	Transverse steel ratio
σ_1^c	Tensile stress in the concrete strut
σ_2^c	Compressive stress in the concrete strut
σ_c	Compressive stress in concrete
σ_{cagg}	Normal stresses due to aggregate interlock
σ_{ct}	Tensile stress in concrete
σ_d	Principal compressive stress in concrete
σ_l	Stress in RC panel in longitudinal direction
σ_r	Principal tensile stress in concrete
σ_t	Stress in RC panel in transverse direction
τ_{12}^c	Shear stresses in the concrete strut
τ_{agg}	Shear stress due to aggregate interlock
τ_{lt}	Shear stress in RC panel in l-t directions
τ_{lt}^s	Dowel stress in reinforcement

10. Copyrights

11. References

[1] Mitchell D, Collins MP (1974): Diagonal compression field theory-a rational model for structural concrete in pure torsion. *ACI Journal Proceedings*, 71(8), 396–408.

[2] Collins MP, Mitchell D (1980): Shear torsion design of prestressed non-prestressed concrete beams. *Journal - Prestressed Concrete Institute*, 25(5), 32–100.

[3] Vecchio FJ, Collins MP (1986): The modified compression-field theory for reinforced concrete elements subjected to shear. *ACI Journal Proceedings*, 83(2), 219–231.

[4] Pang XB, Hsu TTC (1995): Behavior of reinforced concrete membrane elements in shear. *ACI Structural Journal*, 92(6), 665–679.

[5] Pang XB, Hsu TTC (1996): Fixed angle softened truss model for reinforced concrete. *ACI Structural Journal*, 93(2), 197–207.

[6] Vecchio FJ (2000): Disturbed stress field model for reinforced concrete: Formulation. *Journal of Structural Engineering*, 126(9), 1070–1077.

[7] Hsu TTC, Zhu RRH. (2002): Softened membrane model for reinforced concrete elements in shear. *ACI Structural Journal*, 99(4), 460–469.

[8] Kothamuthyala SR, Thammishetti N, Suriya Prakash S, Vyasarayani CP (2019): Optimization-based improved softened-membrane model for rectangular R.C members under combined shear torsion. *Journal of Structural Engineering*, 145(2), 04018259.

[9] Ulugtekin D (2010): *Analytical modeling of reinforced concrete panel elements under reversed cyclic loadings*. (M.S. thesis, Bogazici University).

[10] Orakcal K, Ulugtekin D, Massone LM. (2012): Constitutive modeling of reinforced concrete panel behavior under cyclic loading. *15th World Conference on Earthquake Engineering*, Lisboa.

[11] Kolozvari K, Orakcal K, Wallace JW (2015): Shear-flexure interaction modeling for reinforced concrete structural walls columns under reversed cyclic loading. *Technical Report PEER 2015/12*, PEER, Berkeley, USA.

[12] Chang GA, Mer JB (1994): Seismic energy based fatigue damage analysis of bridge columns: Part I - Evaluation of seismic capacity. *NCEER Technical Report No. NCEER-94-0006*, NCEER, Buffalo, NY.

[13] Belarbi A, Hsu TTC (1994): Constitutive laws of concrete in tension reinforcing bars stiffened by concrete. *ACI Structural Journal*, 91(4), 465–474.

[14] Menegotto M, Pinto PE (1973): Method of analysis for cyclically loaded R.C plane frames including changes in geometry non-elastic behavior of elements under combined normal force bending. *IABSE Symposium on Resistance Ultimate Deformability of Structures Acted on by Well Defined Loads*, 15–22.

[15] Kolozvari K (2013): *Analytical modeling of cyclic shear - flexure interaction in reinforced concrete structural walls*. (Doctoral dissertation, University of California, Los Angeles).

[16] Bujadham B, Maekawa K (1992): The universal model for stress transfer across cracks in concrete. *Proc. of JSCE*, 277–287.

[17] Maekawa K, Pimanmas A, Okamura H. (2003): *Nonlinear mechanics of reinforced concrete*. Taylor & Francis Group, 1st edition.

[18] Zhang LX, Hsu TTC (1998): Behavior analysis of 100 MPa concrete membrane elements. *Journal of Structural Engineering*, 124(1), 24–34.

